Aalborg Universitet

Consistent diurnal pattern of leaf respiration in the light among contrasting species and climates

Faber, Andreas H.; Griffin, Kevin L.; Tjoelker, Mark G.; Pagter, Majken; Yang, Jinyan; Bruhn, Dan

[Link to publication from Aalborg University](#)

Consistent diurnal pattern of leaf respiration in the light among contrasting species and climates

Andreas H. Faber[1] (iD), Kevin L. Griffin[2,3,4] (iD), Mark G. Tjoelker[5] (iD), Majken Pagter[1] (iD), Jinyan Yang[5] (iD) and Dan Bruhn[1] (iD)

[1]Department of Chemistry and Bioscience, Aalborg University, Fredrik Bajers Vej 7H, 9220, Aalborg, Denmark; [2]Department of Earth and Environmental Sciences, Columbia University, Palisades, NY 10964, USA; [3]Department of Ecology, Evolution and Environmental Biology, Columbia University, New York, NY 10027, USA; [4]Lamont-Doherty Earth Observatory, Columbia University, Palisades, NY 10964, USA; [5]Hawkesbury Institute for the Environment, Western Sydney University, Penrith, NSW 2750, Australia

Author for correspondence:
Andreas H. Faber
Email: FaberHavbro@outlook.dk

Summary

- Leaf daytime respiration (leaf respiration in the light, R_L) is often assumed to constitute a fixed fraction of leaf dark respiration (R_D) (i.e. a fixed light inhibition of respiration (R_D)) and vary diurnally due to temperature fluctuations.
- These assumptions were tested by measuring R_L, R_D and the light inhibition of R_D in the field at a constant temperature using the Kok method. Measurements were conducted diurnally on 21 different species: 13 deciduous, four evergreen and four herbaceous from humid continental and humid subtropical climates.
- R_L and R_D showed significant diurnal variations and the diurnal pattern differed in trajectory and magnitude between climates, but not between plant functional types (PFTs). The light inhibition of R_D varied diurnally and differed between climates and in trajectory between PFTs.
- The results highlight the entrainment of leaf daytime respiration to the diurnal cycle and that time of day should be accounted for in studies seeking to examine the environmental and biological drivers of leaf daytime respiration.

Introduction

Terrestrial plants are estimated to fix 120 Gt carbon (C) every year through photosynthesis and roughly 30 Gt C is emitted to the atmosphere through leaf respiration (Prentice *et al.*, 2001). This C efflux is approximately three times larger than current emissions from burning of fossil fuels globally (Canadell *et al.*, 2007; Le Quéré *et al.*, 2009; Friedlingstein *et al.*, 2020). However, current modelling of leaf respiration C fluxes is considered inadequate, leading to uncertain estimates of future climate and vegetation dynamics (Gifford, 2003; Leuzinger & Thomas, 2011; Huntingford *et al.*, 2013; Smith & Dukes, 2013; Lombardozzi *et al.*, 2015).

Inadequate representation of leaf respiration in current modelling approaches is related to incomplete understanding of the environmental and biological controls of leaf daytime respiration (Kruse *et al.*, 2011; Searle *et al.*, 2011; Huntingford *et al.*, 2013; Kornfeld *et al.*, 2013; Tcherkez *et al.*, 2017a,b). Leaf respiration is often measured during the day using darkened chambers (R_D) (Atkin *et al.*, 2015). However, rates of leaf respiration in the light (R_L) are often substantially lower than those in darkness (Amthor & Baldocchi, 2001; Janssens *et al.*, 2001; Morgenstern *et al.*, 2004; Wohlfahrt *et al.*, 2005; Bruhn *et al.*, 2011; Bathellier *et al.*, 2017). Failure to consider this light inhibition of

respiration (R_D) can lead to overestimates of daily respiratory fluxes in individual leaves (Atkin *et al.*, 2006), and thus have implications for our understanding of how environmental and biological factors drive leaf daytime respiration.

The light inhibition of R_D can depend on temperature (Atkin *et al.*, 2000, 2006; Griffin & Turnbull, 2013; Way & Yamori, 2014), drought (Ayub *et al.*, 2011; Crous *et al.*, 2012; Sperlich *et al.*, 2016), CO_2 (Shapiro *et al.*, 2004; Ayub *et al.*, 2014), long-term growth temperature (Heskel *et al.*, 2014; McLaughlin *et al.*, 2014), soil nutrient availability (Heskel *et al.*, 2012; Atkin *et al.*, 2013), season (Way *et al.*, 2015) and plant functional type (PFT) (Heskel *et al.*, 2012, 2014; Crous *et al.*, 2017a). Some approaches account for the light inhibition of R_D by assuming R_L constitutes a fixed fraction of R_D. For example, the terrestrial biosphere model (TBM) Joint UK Land Environmental Simulator (JULES) model assumes R_D is 30% inhibited when light is available (Cox, 2001; Clark *et al.*, 2011). Although several studies demonstrate a mean light inhibition of *c.* 30% (Budde & Randall, 1990; Tcherkez *et al.*, 2005, 2009, 2012b, 2017a; Buckley & Adams, 2011; Heskel *et al.*, 2013; Kroner & Way, 2016), the light inhibition of R_D can vary between 0 and 100% (Atkin *et al.*, 2006; Zaragoza-Castells *et al.*, 2007; Crous *et al.*, 2012; Heskel *et al.*, 2013; Way *et al.*, 2019) and occasionally R_L even exceeds R_D (Zaragoza-Castells *et al.*, 2007; Crous *et al.*, 2017a).

Studying temporal patterns of R_L and R_D could shed light on the validity of the assumption of a fixed proportion of light inhibition of R_D and provide further insight into daytime leaf respiration.

Leaf respiration varies diurnally due to temperature fluctuations and is a key driver in modelled respiration (Running & Coughlan, 1988; Raich et al., 1991; Melillo et al., 1993; Cox, 2001; Clark et al., 2011; Oleson et al., 2013). However, leaf respiration may also be influenced by antecedent conditions. The amount of substrate available for respiration often directly relates to light intensity and photosynthesis (Högberg & Read, 2006). Substrate supply and demand processes for respiration can vary within hours depending on the environment (Trumbore, 2006; Hagedorn et al., 2016; O'Leary et al., 2019). Leaf respiration may also be under circadian regulation as protein expressions of enzymes central to respiration show diurnal rhythmicity (Wijnen & Young, 2006) and some indirect evidence, provided by statistical filtering techniques, shows that daytime net ecosystem CO_2 exchange is affected by circadian regulation (Doughty et al., 2006; Resco de Dios et al., 2012).

If leaf respiration is under circadian regulation, and/or is dependent on previous environmental and leaf physiological conditions, leaf respiration will depend on the time of day even if the temperature is held constant. In addition, as R_L and R_D often respond differently to changes in the growth environment (Atkin et al., 2005; Zaragoza-Castells et al., 2007; McLaughlin et al., 2014; Kroner & Way, 2016; Crous et al., 2017b), time of day could affect R_L and R_D differently. Given that the environment differs significantly between climates, and that rhythms in plant physiological processes are entrained by environmental cues such as light and temperature (Resco de Dios & Gessler, 2018), the effect of time of day on leaf respiration may vary between climates.

Respiratory fluxes differ among cooccurring species and PFTs under field conditions (Bolstad et al., 2003; Tjoelker et al., 2005; Turnbull et al., 2005; Heskel et al., 2012, 2014; Slot et al., 2013; Crous et al., 2017a) and under controlled environments (Reich et al., 1998; Loveys et al., 2003; Xiang et al., 2013), suggesting strong genetic control of respiratory fluxes. Hence, effects of time of day on R_L, R_D and the light inhibition of R_D may be a function of PFTs and species. The consequences of time of day on leaf respiration and the magnitude of effects are currently unknown and could potentially be an important source of variation in leaf respiration. If true, time of day should be accounted for in measurements and models of respiration.

The aim of this study was to examine whether leaf daytime R_D, R_L and the light inhibition of R_D exhibit diurnal variation when measured at a constant temperature in the field, and to determine whether this diurnal variation differs between climates and PFTs. The measurements were conducted using the Kok method (Kok, 1948) on 21 different species, including 13 deciduous, four evergreen and four herbaceous species from two contrasting climates: a humid continental and a humid subtropical. The validity of the Kok method as a reliable estimator of R_L has been under much debate (Buckley et al., 2017; Farquhar & Busch, 2017; Gauthier et al., 2020; Yin et al., 2020) as estimates of R_L using the method are influenced by increasing CO_2 concentrations at the sites of carboxylation (C_c), caused by decreasing stomatal conductance (g_s) and mesophyll conductance (g_m) at decreasing irradiance levels, and by changes in the quantum yield (ϕPsII) (Yin et al., 2011; Farquhar & Busch, 2017). However, the Kok method is currently viewed as a proxy for R_L (Gauthier et al., 2020; Yin et al., 2020), and was used here because of its field applicability compared to other methods, and because over 800 published papers have used or cited the method, which is c. 40% of all studies involved with daytime respiration (Tcherkez et al., 2017a). It was hypothesized that: the basal rate of R_L, R_D and the light inhibition of R_D, estimated with the Kok method, exhibit diurnal variations when measured at constant leaf temperature in the field; and the diurnal variations of the basal rate of R_L, R_D and the light inhibition of R_D, estimated with the Kok method, are different between climates and PFTs.

Materials and Methods

Study sites and climate conditions

The study took place in Denmark and Australia from 2019 to 2021. The measurements conducted in Denmark were collected from 31 August 2019 to 12 October 2019 in a mixed deciduous forest in northern Jutland (56°45′32″N, 10°12′4″E, 8 m above sea level (asl)) and again from 30 July 2021 to 30 August 2021 in another nearby mixed deciduous forest (56°40′59″N, 10°10′34″E, 20 m asl). The soil is a glacial outwash plain at both locations. In Australia, the measurements were conducted at the Hawkesbury Forest Experiment (HFE) site in Richmond, New South Wales (33°36′40″S, 150°44′26.5″E, 30 m asl) from 11 January 2020 to 29 February 2020 where the soil consists of a low-fertility sandy loam (Drake et al., 2016). The climate at the Danish study sites is humid continental while the climate at the Australian study site is humid subtropical. Precipitation and temperature data from 2011 to 2021 and during the time of data collection can be found in the supplementary site description for the region covering the Danish study sites (Supporting Information Notes S1 Fig. A–B and G–J, respectively) and the study site in Australia (Notes S1 Fig. C–D and E–F, respectively). In total, 18 mm of rain fell in the summer period from the start of November 2019 to start of January 2020 at the study site in Australia, resulting in a significant dry period before the study period. Watering with cleaned wastewater every fourth day occurred at the study site in Australia for a subset of the measured species (Table S1).

Species selection

Twenty-one species in total, representing three PFTs, were included in the study: 13 deciduous tree species, four evergreen tree species and four herbaceous species, 10 of which were measured in Denmark, and the remainder in Australia (Table S1). For each species, measurements were only performed on

individuals which on clear days were exposed to direct sunlight throughout most of the day.

Leaf gas exchange measurements

Measurements of leaf net CO_2 exchange (A_{net}, µmol CO_2 m^{-2} s^{-1}), stomatal conductance for water vapour (g_{sw}, mol m^{-2} s^{-1}) and respiration in the dark were conducted on newly developed, fully expanded sun-adapted leaves 0.1–2 m above ground level. Each leaf was measured 3–11 times throughout a single day, usually before sunrise until after sunset with a period of 35 min to 1 h in between each measurement. The measurements were conducted on at least four replicate plants (one leaf per plant) of each species under varying weather conditions (variation in precipitation, cloud cover, wind and temperature). The leaves within species were selected based on morphological similarity.

The measurements were conducted using a Li-Cor 6800 portable photosynthesis system (Li-Cor, Lincoln, NE, USA) with a 6 cm^2 leaf chamber and a 6800-01A fluorometer set to 69% red and 31% blue light. On each measurement day, leaf temperature was preset to a constant temperature (T_o). For the measurements conducted in 2019 in Denmark T_o was set to match the median air temperature of the day based on weather forecasts, whereas T_o was set a few degrees below the maximum daily air temperature for the measurements in Australia in 2020 and Denmark in 2021. Hence, T_o varied between leaves both within and between all measured species but was kept constant within each leaf repeatedly measured throughout the day. The measurements were conducted using the Kok method with a relative air humidity of 35–80%, a flow rate of 300–350 µmol s^{-1}, a fan speed of 10 000 rpm and a CO_2 concentration of 410 ppm in the leaf chamber. The leaf irradiance response of A_{net} was measured from 100 µmol photons m^{-2} s^{-1} down to 0 µmol photons m^{-2} s^{-1} in steps of 10–12 irradiance levels. Before measuring A_{net} at each irradiance level, the reference and sample infrared gas analysers (IRGAs) were automatically matched, and gas exchange fluxes were given 2–5 min to stabilize. The stabilizing period for the 0 µmol photons m^{-2} s^{-1} irradiance level was increased to 10 min. Gas exchange fluxes were allowed to stabilize before initiation of the light response curve. This stabilization typically required 2–20 min.

Calculation of leaf light and dark respiration

The Kok method was used to calculate R_L (µmol CO_2 m^{-2} s^{-1}) while R_D (µmol CO_2 m^{-2} s^{-1}) was measured following leaf dark adaptation. The apparent R_L was estimated based on the intercept of a linear regression fitted to the linear region above the Kok effect and R_D was determined directly from the CO_2 efflux in the dark. When using the Kok method, intercellular CO_2 concentration (C_i, µmol mol^{-1}) tends to increase as irradiance decreases, resulting in reduced photorespiration and increased carboxylation (Villar *et al.*, 1994). As a result, the slope of A_{net} light response curves tends to decrease, resulting in the concurrent underestimation of R_L (Kirschbaum & Farquhar, 1987; Villar *et al.*, 1994).

Accordingly, rates of R_L were corrected for changes in C_i by iteratively forcing the intercept of the quantum yield of RuP$_2$ regeneration, V_j, against irradiance through the origin. Following this, $V_j - R_L$ was plotted against irradiance and a linear regression was fitted to the linear region above the Kok effect and extrapolated to the *y*-axis yielding the actual R_L (Fig. S1). V_j was calculated following Kirschbaum & Farquhar (1987):

$$V_j = \frac{(A_{net} + R_L) \cdot \left(1 + \frac{2\Gamma^*_{leafT}}{C_i}\right)}{1 - \frac{\Gamma^*_{leafT}}{C_i}} \qquad \text{Eqn 1}$$

where Γ^* (µbar) is the apparent CO_2 compensation point in the absence of R_L (von Caemmerer & Farquhar, 1981) and A_{net} is the rate of net CO_2 exchange at any given irradiance. The C_i-based Γ^* at 25°C ($\Gamma^*_{25°C}$) was assumed to be 38.6 µbar for all species, and Γ^* at any given leaf temperature (Γ^*_{leafT}) can be calculated according to Brooks & Farquhar (1985):

$$\Gamma^*_{leafT} = \Gamma^*_{25°C} + 1.88 \left(T_{leaf} - 25\right) + 0.036 \left(T_{leaf} - 25\right)^2. \qquad \text{Eqn 2}$$

The C_i-corrected R_L and the R_D estimated from the CO_2 efflux in the dark was subsequently used to calculate the % light inhibition of R_D as $1 - (R_L/R_D)100$. The rate of gross photosynthesis (A_{gross}, µmol CO_2 m^{-2} s^{-1}) was calculated as $R_{L,To}$ plus A_{net} at the 100 µmol photons m^{-2} s^{-1} irradiance level.

Data analysis

To examine whether R_L and R_D exhibited diurnal variation measured at a constant temperature (hereafter denoted as $R_{L,To}$ and $R_{D,To}$), all measurements of $R_{L,To}$ and $R_{D,To}$ were standardized by dividing each measurement from a single leaf by the mean $R_{L,To}$ or $R_{D,To}$ measurement of that leaf (i.e. $R_{L,To}/\overline{R_{L,To}}$ and $R_{D,To}/\overline{R_{D,To}}$, respectively). Diurnal variations in $R_{L,To}/\overline{R_{L,To}}$ and $R_{D,To}/\overline{R_{D,To}}$, as well as the % light inhibition of $R_{D,To}$ were examined using generalized additive models (GAMs) with 95% pointwise confidence intervals fitted with automated smoothness selection in the MGCV library in R v.4.1.0 (R Core Team, 2021) with RSTUDIO v.1.4.1717 (R Studio Team, 2021), using restricted maximum likelihood (REML) (Wood, 2017). The GAMs had the following components:

$$y_i = \alpha + f(x_i) + \epsilon_i \qquad \text{Eqn 3}$$

where y_i is the observation at time x_i, α is the intercept, $f(x_i)$ is a smooth function and ϵ_i is the residual error. This approach is nonparametric and makes no *a priori* assumption about the functional relationship between variables (Wood, 2017), allowing the depiction of the empirical trend of $R_{L,To}/\overline{R_{L,To}}$ and $R_{D,To}/\overline{R_{D,To}}$ and the % light inhibition of $R_{D,To}$ over time without restrictions. The residual variation was assumed to follow a gaussian distribution, and the residual autocorrelation was modelled by a continuous time first-order autoregressive process structure nested within each measured leaf (Pinheiro & Bates, 2000).

Accordingly, GAMs by the formulation of Eqn 3 were fitted to $R_{L,To}/\overline{R_{L,To}}$ and $R_{D,To}/\overline{R_{D,To}}$ and % light inhibition of $R_{D,To}$ measurements across all measurements, across measurements within climates (i.e. Australia and Denmark), within PFTs and within species. As the $R_{L,To}/\overline{R_{L,To}}$, $R_{D,To}/\overline{R_{D,To}}$ and the % light inhibition of $R_{D,To}$ measurements in Denmark were represented by nine deciduous tree species and one herbaceous species, the fitting of GAMs to PFTs was restricted to Australia. Significant diurnal variations of $R_{L,To}/\overline{R_{L,To}}$, $R_{D,To}/\overline{R_{D,To}}$ and the % light inhibition of $R_{D,To}$ were determined after computation of the first derivative (the slope) of the fitted GAMs with the finite differences method. The first derivatives were computed with 95% pointwise confidence intervals, and the trend was deemed significant when the derivative confidence interval was bounded away from zero at the 95% level (for more details on this method, see Curtis & Simpson, 2014). The percentage total diurnal variation was calculated from the difference between minimum and maximum predicted values of $R_{L,To}/\overline{R_{L,To}}$, $R_{D,To}/\overline{R_{D,To}}$ and the % light inhibition of $R_{D,To}$, divided by the maximum GAM-predicted values.

Model selection was used to determine whether the diurnal variation in $R_{L,To}/\overline{R_{L,To}}$, $R_{D,To}/\overline{R_{D,To}}$ and % light inhibition of $R_{D,To}$ differed between climates and PFTs (Wieling, 2018). Models with the structure of Eqn 3 or with PFT or climate added as a covariate (Eqn 4) and an interaction term (Eqn 5) were fitted across climates or across all three PFTs in Australia using the following equations:

$$y_i = \alpha + f(x_i) + K_i + \epsilon_i \qquad \text{Eqn 4}$$

$$y_i = \alpha + f(x_i) + K_i + f(x_i) \times k_{1,i} + \ldots + f(x_i) \times k_{n,i} + \epsilon_i \qquad \text{Eqn 5}$$

where K is a categorical variable (i.e. climate or PFT) of n levels ($k_1 - k_n$). The variable $k_{n,i}$ is 1 if an observation is from level k_n, and otherwise 0. The models explaining the highest variance with the minimum number of variables were identified using Akaike's information criterion (AIC).

The prediction of $R_{L,To}/\overline{R_{L,To}}$, $R_{D,To}/\overline{R_{D,To}}$ and the % light inhibition of $R_{D,To}$ from physiological and external environmental variables was examined using linear or logarithmic regression models with 95% pointwise confidence intervals. The ambient temperature (°C), light intensity (µmol m^{-2} s^{-1}) and water vapour pressure deficit (VPD; kPa), provided by the climate station at HFE in Australia, were averaged for every hour during the time of measuring a light response curve of A_{net}. Model assumptions of normality and homoscedasticity of residuals were assessed and verified before analysis.

To examine the potential error of assuming a constant rate of $R_{L,To}$ throughout a day, the GAMs that were initially fitted to the $R_{L,To}/\overline{R_{L,To}}$ values were used to predict $R_{L,To}$ throughout a day based on a hypothetical scenario, where an $R_{L,To}$ measurement of 0.76 µmol CO_2 m^{-2} s^{-1} (i.e. the mean estimated $R_{L,To}$ value across all species in this study) was measured at 08:00 h. Accordingly, temporal GAMs at constant temperature were fitted to the $R_{L,To}/\overline{R_{L,To}}$ values from Australia and Denmark using Eqn 3. However, for these models we estimated 95% simultaneous confidence intervals from the multivariate normal distribution of the models that contain 95% of the posterior draws from the estimated models, according to Simpson (2018). Subsequently, these models were used to predict the $R_{L,To}$ measurement of 0.76 µmol CO_2 m^{-2} s^{-1} at other times of the day following:

$$R_{L,To\,i} = R_{L,To} \times \left(\frac{\alpha + f(\text{time}_i) + \epsilon_i}{\alpha + f(\text{time}_x) + \epsilon_x} \right) \qquad \text{Eqn 6}$$

where $R_{L,To\,i}$ is the predicted rate of respiration at constant temperature at time$_i$. $R_{L,To}$ is the measured $R_{L,To}$ (0.76 µmol CO_2 m^{-2} s^{-1}) at time$_x$ (08:00 h), ϵ_x is the residual error at time$_x$ and ϵ_i is the residual errors at time$_i$. Null models (i.e. linear regression models without a slope) were fitted through the maximum, mean and minimum predicted values of the temporal GAMs for Australia and Denmark, and the predicted accumulated CO_2 throughout a day was calculated for each model. The percentage predicted difference in accumulated CO_2 between the maximum, mean and minimum models compared to the temporal GAMs was subsequently calculated. Eqn 6 was further merged with a Q_{10} model in order to calculate $R_{L,T}$ (i.e. R_L under varying temperature conditions):

$$R_{L,T\,i} = \left(R_{L,To} \times \left(\frac{\alpha + f(\text{time}_i) + \epsilon_i}{\alpha + f(\text{time}_x) + \epsilon_x} \right) \right) \times 2^{\left(\frac{(T_i - T_o)}{10} \right)} \qquad \text{Eqn 7}$$

where 2 denotes the factor by which $R_{L,T\,i}$ changes for every 10°C temperature change, $R_{L,T\,i}$ is the predicted rate of respiration at temperature T_i and T_o is the temperature at the time where $R_{L,To}$ was measured. Using Eqn 7, $R_{L,T}$ (i.e. R_L at different temperatures) was calculated at three different temperature profiles for both climates. A parametric approach with quadratic linear regression models and 95% pointwise confidence intervals was also constructed following:

$$R_{L,T\,i} = \left(R_{L,To} \times \left(\frac{\alpha + \beta\text{time}_i + \beta_1\text{time}_i^2 + \epsilon_i}{\alpha + \beta\text{time}_x + \beta_1\text{time}_x^2 + \epsilon_x} \right) \right) \times 2^{\left(\frac{(T_i - T_o)}{10} \right)} \qquad \text{Eqn 8}$$

where α is the model intercept, β and β_1 are model coefficients, and ϵ indicates the residuals, which are assumed to follow a gaussian distribution. Using the guide in Dataset S1 and the R script (Notes S2), an $R_{L,To}$ measurement from any time of the day can be used to predict $R_{L,T}$ or $R_{L,To}$ with either GAMs or quadratic linear regression models throughout the day depending on whether the daily temperature is constant or varying. The temperature profiles were derived from the ambient air temperature during the time of measuring the light response curves in Australia. Quadratic linear regression models were fitted through the maximum, mean and minimum temperature within 2 h intervals from 04:00 to 22:00 h from these data, yielding three different temperature profiles, respectively, which can be viewed in Fig. S2.

Results

Diurnal variation in leaf light and dark respiration

When standardizing $R_{L,To}$ and $R_{D,To}$ at the individual leaf level, $R_{L,To}/\overline{R_{L,To}}$ and $R_{D,To}/\overline{R_{D,To}}$ increased significantly from sunrise until morning or early midday, stabilized and then decreased significantly from late midday until sunset (Figs 1a,b, S3). Although $R_{L,To}/\overline{R_{L,To}}$ and $R_{D,To}/\overline{R_{D,To}}$ showed significant variations at approximately the same time of day, the total diurnal variation in the fitted models was larger for $R_{L,To}/\overline{R_{L,To}}$ compared to $R_{D,To}/\overline{R_{D,To}}$ (38% and 12% change, respectively, Table S2). In addition, the diurnal patterns showed no linear association with the various preset constant leaf measurement temperatures

($r^2 = 1.234667 \times 10^{-29}$, $P > 0.05$ and $r^2 = 3.505181 \times 10^{-30}$, $P > 0.05$, for $R_{L,To}/\overline{R_{L,To}}$ and $R_{D,To}/\overline{R_{D,To}}$, respectively) (Fig. S4), showing that the diurnal patterns were persistent across a wide range of leaf temperatures.

The diurnal variation of $R_{L,To}/\overline{R_{L,To}}$ and $R_{D,To}/\overline{R_{D,To}}$ persisted when analysing measurements within climates, and this pattern differed between the climates for both $R_{L,To}/\overline{R_{L,To}}$ and $R_{D,To}/\overline{R_{D,To}}$ (Fig. 1a,b; Table S3). For Australia, $R_{L,To}/\overline{R_{L,To}}$ increased significantly from sunrise until morning, stabilized and then decreased significantly from early midday until sunset (Fig. 1a). By contrast, $R_{D,To}/\overline{R_{D,To}}$ was stable from sunrise until early midday, and then decreased significantly until sunset (Fig. 1b). In addition, $R_{L,To}/\overline{R_{L,To}}$ exhibited a larger total variation in the fitted model compared to $R_{D,To}/\overline{R_{D,To}}$ (45% and 24% change,
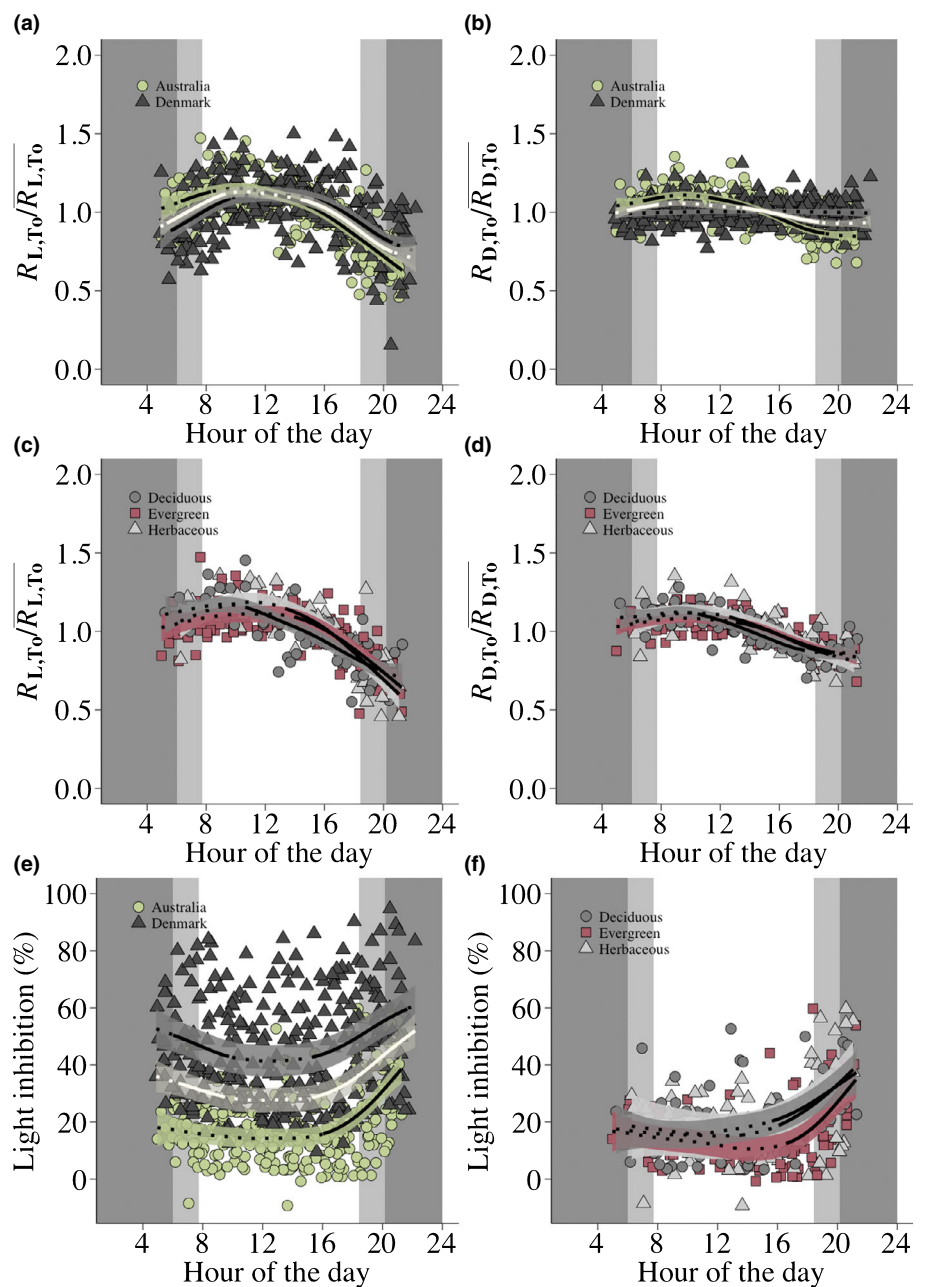
Fig. 1 The diurnal variation of (a, c) leaf respiration in the light ($R_{L,To}/\overline{R_{L,To}}$), (b, d) leaf dark respiration ($R_{D,To}/\overline{R_{D,To}}$) and (e, f) the % light inhibition of leaf respiration ($1 - (R_{L,To}/R_{D,To})100$). Generalized additive models (GAMs) with 95% pointwise confidence intervals are fitted across (a, b, e) measurements of 10 field-grown plant species from Denmark (dark triangles, $n = 295$), 11 from Australia (green circles, $n = 270$) and across (c, d, f) four deciduous (dark circles, $n = 88$), four evergreen (red squares, $n = 115$) and three herbaceous (grey triangles, $n = 65$) species measured in Australia. GAMs indicated by the white lines in (a, b, e) are fitted across all measurements from Denmark and Australia ($n = 562$). Since the measurements from Denmark were represented by nine deciduous and one herbaceous species, the fitting of GAMs to PFTs was restricted to the measurements in Australia where four deciduous, four evergreen and three herbaceous species were measured. Significant variations in the diurnal variation of $R_{L,To}/\overline{R_{L,To}}$, $R_{D,To}/\overline{R_{D,To}}$ and the % light inhibition of leaf respiration are indicated by the solid portions of the fitted GAMs while dotted portions illustrate nonsignificant variations. Dark shaded areas illustrate night-time shared for all days of measuring and light shaded areas illustrate the variation in time of sunrise and sunset between the days of measuring. The studied species are detailed in Supporting Information Table S1.

respectively, Table S2). In Denmark, $R_{L,To}/\overline{R_{L,To}}$ increased significantly from sunrise until early midday, stabilized and then decreased significantly from late midday until sunset (Fig. 1a) and the total variation in the fitted model was comparable to that of $R_{L,To}/\overline{R_{L,To}}$ in Australia (33% change, Table S2). By contrast, $R_{D,To}/\overline{R_{D,To}}$ did not exhibit a significant diurnal variation in Denmark, but remained stable throughout the day with only minimal total variation in the fitted model (Fig. 1b; Table S2). All measured species in Australia exhibited significant diurnal variations in $R_{L,To}/\overline{R_{L,To}}$ and $R_{D,To}/\overline{R_{D,To}}$ (Figs S5–S7). In Denmark, eight out of 10 species exhibited significant diurnal variations in $R_{L,To}/\overline{R_{L,To}}$, while five exhibited significant diurnal variations in $R_{D,To}/\overline{R_{D,To}}$ (Figs S8–S10).

The PFTs measured in Australia showed similar diurnal variations in both $R_{L,To}/\overline{R_{L,To}}$ and $R_{D,To}/\overline{R_{D,To}}$ (Fig. 1c,d; Table S3). For each PFT, $R_{L,To}/\overline{R_{L,To}}$ and $R_{D,To}/\overline{R_{D,To}}$ were stable from sunrise until early or late midday, and decreased significantly until late evening or sunset (Fig. 1c,d). The total variation in the fitted models for $R_{L,To}/\overline{R_{L,To}}$ and $R_{D,To}/\overline{R_{D,To}}$ was of similar magnitude between the PFTs (Deciduous: 40% and 21% change, Evergreen: 42% and 23% change, Herbaceous: 49% and 28% change, respectively, Table S2), although the total variation of $R_{L,To}/\overline{R_{L,To}}$ was slightly larger than that of $R_{D,To}/\overline{R_{D,To}}$ for all PFTs.

Diurnal variation in the light inhibition of $R_{D,To}$

Across climates, the light inhibition of $R_{D,To}$ decreased significantly from sunrise until morning, stabilized and then increased significantly from late midday until sunset (Fig. 1e). The variation in the inhibition values ranged between −9% and 95% with a mean inhibition of 32% (Table S4) and the total variation in the fitted model was 47% (Table S2), emphasizing that $R_{L,To}$ and $R_{D,To}$ exhibited different diurnal patterns.

The diurnal variation of the light inhibition of $R_{D,To}$ differed between the climates (Fig. 1e; Table S3). For Denmark, the light inhibition of $R_{D,To}$ decreased significantly from sunrise until morning, stabilized and then increased significantly from late midday until sunset (Fig. 1e). For Australia, the light inhibition of $R_{D,To}$ was stable from sunrise until late midday, and then increased significantly from late midday until sunset (Fig. 1e). The total variation in the fitted model for Denmark was 32% and the mean inhibition was 45% (Tables S2, S4) while the total variation in the fitted model for Australia was 63% and the mean inhibition was 18% (Tables S2, S4, respectively). In addition, the variation in the inhibition values was larger for Denmark than for Australia (Fig. 1e; Table S4).

The diurnal variation of the light inhibition of $R_{D,To}$ differed between the PFTs measured in Australia (Fig. 1f; Table S3). For each PFT, the light inhibition of $R_{D,To}$ was stable from sunrise until late midday or evening, and then increased significantly until sunset (Fig. 1f). However, the evergreen PFT showed a more abrupt increase in the evening compared to the other PFTs. In addition, the total variation in the fitted models was 58%, 70% and 61% for the deciduous, evergreen and herbaceous PFT,

respectively (Table S2), and the mean and range in inhibition were similar among the three (Table S4).

### Importance of photosynthetic rate and stomatal conductance

There was a significant positive linear relationship between $R_{L,To}/\overline{R_{L,To}}$ and A_{gross} at the 100 µmol photons m^{-2} s^{-1} irradiance level for the measurements collected in Australia ($r^2 = 0.39$, $P < 0.05$) and for the measurements collected in Denmark ($r^2 = 0.14$, $P < 0.05$) (Fig. 2a). A_{gross} showed a significant positive linear relationship with the $R_{D,To}/\overline{R_{D,To}}$ measurements from Australia ($r^2 = 0.24$, $P < 0.05$) while there was no significant association between A_{gross} and the $R_{D,To}/\overline{R_{D,To}}$ measurements from Denmark ($r^2 = 0.006$, $P > 0.05$) (Fig. 2b). A_{gross} showed a significant positive logarithmic relationship with g_{sw} for the measurements collected in Australia ($r^2 = 0.71$, $P < 0.05$) and for the measurements in Denmark ($r^2 = 0.35$, $P < 0.05$) while g_{sw} was in general higher in Denmark (Fig. S11). The light inhibition of $R_{D,To}$ showed a negative linear association with A_{gross} in Australia ($r^2 = 0.30$, $P < 0.05$) and in Denmark (Fig. S12a) ($r^2 = 0.04$, $P < 0.05$).

Influence of external environmental factors on the diurnal patterns of leaf light and dark respiration

There was a significant positive logarithmic relationship between the ambient light intensity and the $R_{L,To}/\overline{R_{L,To}}$ ($r^2 = 0.49$, $P < 0.05$) and $R_{D,To}/\overline{R_{D,To}}$ ($r^2 = 0.36$, $P < 0.05$) measurements in Australia, such that when the ambient light intensity exceeded c. 100 µmol photons m^{-2} s^{-1} there was no apparent influence of the ambient light intensity on the $R_{L,To}/\overline{R_{L,To}}$ and $R_{D,To}/\overline{R_{D,To}}$ measurements (Fig. 2c,d). In a similar manner, the light inhibition of $R_{D,To}$ showed a logarithmic relationship with ambient light intensity although here the relationship was negative ($r^2 = 0.21$, $P < 0.05$). In addition, ambient temperature and VPD displayed no relationship with the $R_{L,To}/\overline{R_{L,To}}$ and $R_{D,To}/\overline{R_{D,To}}$ measurements (Figs S13a,b, S14a,b).

Error of assuming a constant daytime respiration at constant temperature for modelling integrated respiratory carbon flux in leaves

A hypothetical $R_{L,To}$ value of 0.76 µmol CO_2 m^{-2} s^{-1} (the mean $R_{L,To}$ of this study) measured at 08:00 h was used to predict $R_{L,To}$ throughout the day at a constant temperature for both Australia and Denmark (i.e. temporal models), as described in Eqn 6 (Fig. 3a,d). In addition, models assuming a constant $R_{L,To}$ throughout the day were fitted to the maximum, mean and minimum $R_{L,To}$ values predicted by the temporal models (Fig. 3a,d). For Australia, the predicted daily accumulated CO_2 efflux using the temporal, maximum, mean and minimum models was 40, 46, 40 and 25 mmol m^{-2} d^{-1}, respectively (Fig. 3b). For Denmark, the predicted daily accumulated CO_2 efflux was 46, 52, 46 and 35 mmol m^{-2} d^{-1}, respectively (Fig. 3e). For Australia, the percentage difference in accumulated CO_2 between the
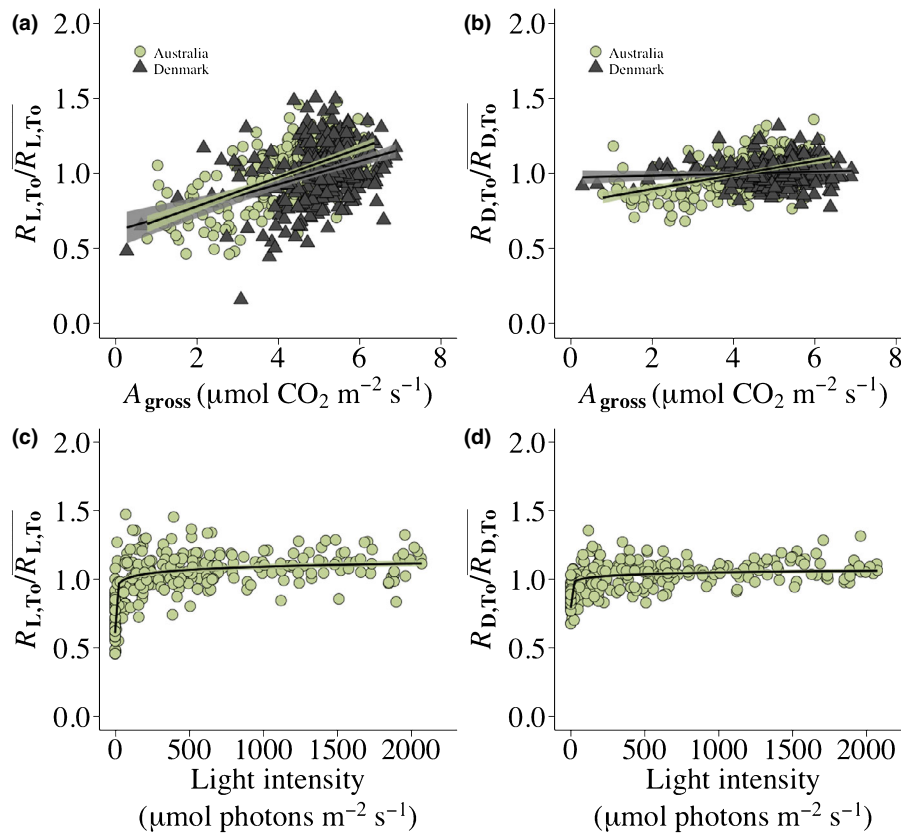
Fig. 2 Leaf respiration (a) in the light ($R_{L,To}/\overline{R_{L,To}}$) and (b) leaf dark respiration ($R_{D,To}/\overline{R_{D,To}}$) measurements conducted in Australia (green circles, $n = 268$) and Denmark (dark triangles, $n = 294$) plotted against A_{gross} (µmol CO_2 m^{-2} s^{-1}) at the 100 µmol photons m^{-2} s^{-1} irradiance level. Leaf respiration (c) in the light ($R_{L,To}/\overline{R_{L,To}}$) and (d) leaf dark respiration ($R_{D,To}/\overline{R_{D,To}}$) measurements conducted in Australia plotted against the recorded mean ambient light intensity (µmol photons m^{-2} s^{-1}) during the time of measuring the light response curves. Linear regression models with 95% pointwise confidence intervals are fitted to the (a) $R_{L,To}/\overline{R_{L,To}}$ ($y_i = 0.581728 + 0.096533A_{gross_i} + \epsilon_i$, $r^2 = 0.39$, $P < 0.05$ and $y_i = 0.61213 + 0.07729A_{gross_i} + \epsilon_i$, $r^2 = 0.14$, $P < 0.05$), (b) $R_{D,To}/\overline{R_{D,To}}$ ($y_i = 0.796791 + 0.046899A_{gross_i} + \epsilon_i$, $r^2 = 0.24$, $P < 0.05$ and $y_i = 0.967332 + 0.006510A_{gross_i} + \epsilon_i$, $r^2 = 0.006$, $P > 0.05$) measurements in Australia and Denmark, respectively. Logarithmic regression models with 95% pointwise confidence intervals are fitted to the (c) $R_{L,To}/\overline{R_{L,To}}$ ($y_i = 0.858178 + 0.033641\log_e(\text{light}_i) + \epsilon_i$, $r^2 = 0.49$, $P < 0.05$) and (d) $R_{D,To}/\overline{R_{D,To}}$ ($y_i = 0.924902 + 0.017814\log_e(\text{light}_i) + \epsilon_i$, $r^2 = 0.36$, $P < 0.05$) measurements in Australia. The studied species are detailed in Supporting Information Table S1.

maximum, mean and minimum models and the temporal model was 14%, −0.09% and −37%, respectively (Fig. 3c), while for Denmark, the percentage difference was 12%, −0.1% and −24%, respectively (Fig. 3f). Hence, the magnitude and direction of the error resulting from assuming a constant rate of $R_{L,To}$ throughout a day is highly dependent on the time of measurement.

Daytime respiration at varying and constant temperature

The predicted diurnal variation of $R_{L,To}$ using the temporal GAMs was compared to the predicted diurnal variation of $R_{L,T}$ had the leaf temperature varied with a maximum, mean and minimum air temperature profile (Fig. 4a,d). For Australia, the predicted accumulated CO_2 for the temporal model (at constant temperature) and the maximum, mean and minimum temperature profile models was 40, 57, 45 and 41 mmol m^{-2} d^{-1}, respectively (Fig. 4b) while for Denmark, the predicted accumulated CO_2 was 46, 67, 52 and 47 mmol m^{-2} d^{-1}, respectively (Fig. 4e). For Australia, the percentage difference in accumulated CO_2 between the maximum, mean and minimum temperature

profile models and the temporal model was 44%, 13% and 2%, respectively (Fig. 4c). For Denmark, this difference was 46%, 14% and 2%, respectively (Fig. 4f). Figures for the same analysis using quadratic linear regression models can be found in Fig. S15.

Discussion

R_L and R_D measured with the Kok method varies over the course of the day at constant measuring temperature

This study shows that leaf daytime respiration exhibits a consistent temporal pattern throughout the day when measured at constant temperature with the Kok method across 21 different plant species, two different climates and three different PFTs, emphasizing the generality of the phenomenon. Leaf daytime respiration is thus clearly driven by time of day, when estimated as both R_L and R_D. Assuming a constant rate of R_L at constant temperature can result in the over- or underestimation of the accumulated daily $R_{L,To}$ by 14% and −37% or 12% and −24%
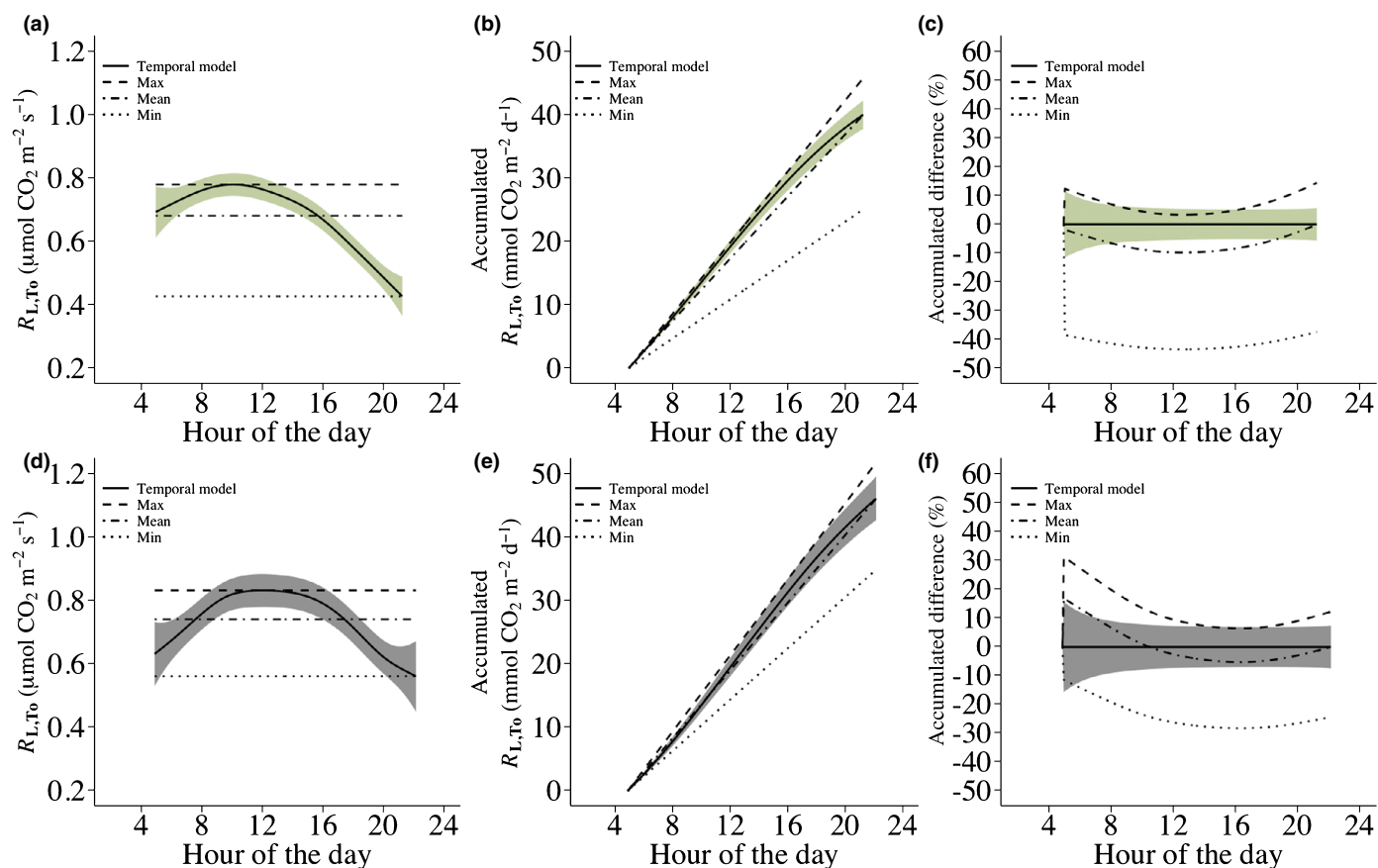
Fig. 3 Temporal generalized additive models (GAMs) of respiration in the light at constant temperature ($R_{L,To}$) for Australia (a) and Denmark (d), where a hypothetical $R_{L,To}$ value of 0.76 μmol CO_2 m^{-2} s^{-1} (i.e. the mean estimated $R_{L,To}$ value across all species in this study) measured at 08:00 h was used to predict $R_{L,To}$ values throughout the day at a constant temperature (solid line) with shaded 95% simultaneous confidence bands. The maximum, mean and minimum models (dashed, dot dashed and dotted lines, respectively) are fitted through the maximum, mean and minimum predicted values of the temporal GAMs, respectively, and assume a constant rate of $R_{L,To}$ throughout the day. The predictions were derived by fitting GAMs to the $R_{L,To}/\overline{R_{L,To}}$ measurements from Australia and Denmark. Subsequently, the hypothetical $R_{L,To}$ value measured at 08:00 h was used to predict $R_{L,To}$ throughout the day from the fitted GAM from Australia as: $R_{L,To_i} = 0.76((0.998728 + f(time_i) + \epsilon_i)/(0.998728 + f(time_x) + \epsilon_x))$ and from the fitted GAM from Denmark as: $R_{L,To_i} = 0.76((1.00074 + f(time_i) + \epsilon_i)/(1.00074 + f(time_x) + \epsilon_x))$, where 0.76 is the $R_{L,To}$ value measured at 08:00 h (time$_x$), ϵ_x is the estimated residual error at 08:00 h, R_{L,To_i} is the predicted rate of respiration at time points time$_i$ and ϵ_i is the residual error at time$_i$. (b, e) Daily accumulated CO_2 efflux predicted by the temporal, max, mean and min models for Australia and Denmark, respectively. (c, f) Percentage difference between accumulated CO_2 predicted by the maximum, mean and minimum models and the temporal models for Australia and Denmark, respectively.

on a diurnal scale as demonstrated for Australia and Denmark, respectively (Fig. 3c,f). This variation in R_L is of similar magnitude to that of the variation in R_L attributed to other studied factors (e.g. CO_2: 32% (Ayub *et al.*, 2014), nutrient availability: 29% (Crous *et al.*, 2017a), drought: *c.* 52–60% (Ayub *et al.*, 2011; Crous *et al.*, 2012), canopy height: 52% (Weerasinghe *et al.*, 2014), seasonality: 32% (Crous *et al.*, 2017b) and temperature: −15 to 90% per every 10°C temperature increase (Atkin *et al.*, 2005)). Errors rising when comparing rates of respiration sampled at different times of the day could potentially bias conclusions on the influence of such effects. Hence, time of day should be accounted for when estimating the response of R_L and R_D to variation in other factors (e.g. temperature and species), or when pooling data across studies even when measurements are performed with the same temperature. Effects of time of day may result in variations of $R_{L,To}$ that in turn affect the calculation of photosynthetic parameters important for

photosynthetic modelling. These could include estimates of maximum carboxylase (V_{cmax}) rates estimated with the one-point A_{sat} method, which has been shown to be sensitive to the chosen R_L (De Kauwe *et al.*, 2016) and thereby affected by time of day.

Light inhibition of $R_{D,To}$ exhibited significant diurnal variations

The light inhibition of $R_{D,To}$ exhibited significant diurnal variations with inhibition values ranging from −9% to 95% and with a mean of 32%, reflecting that the diurnal pattern differed between $R_{L,To}/\overline{R_{L,To}}$ and $R_{D,To}/\overline{R_{D,To}}$. This indicates that R_L and R_D are regulated by different processes, as supported by ample biochemical evidence (Hurry *et al.*, 2005; Tcherkez *et al.*, 2010, 2012a, 2017b) and by studies showing that the temperature sensitivity of R_L may differ from that of
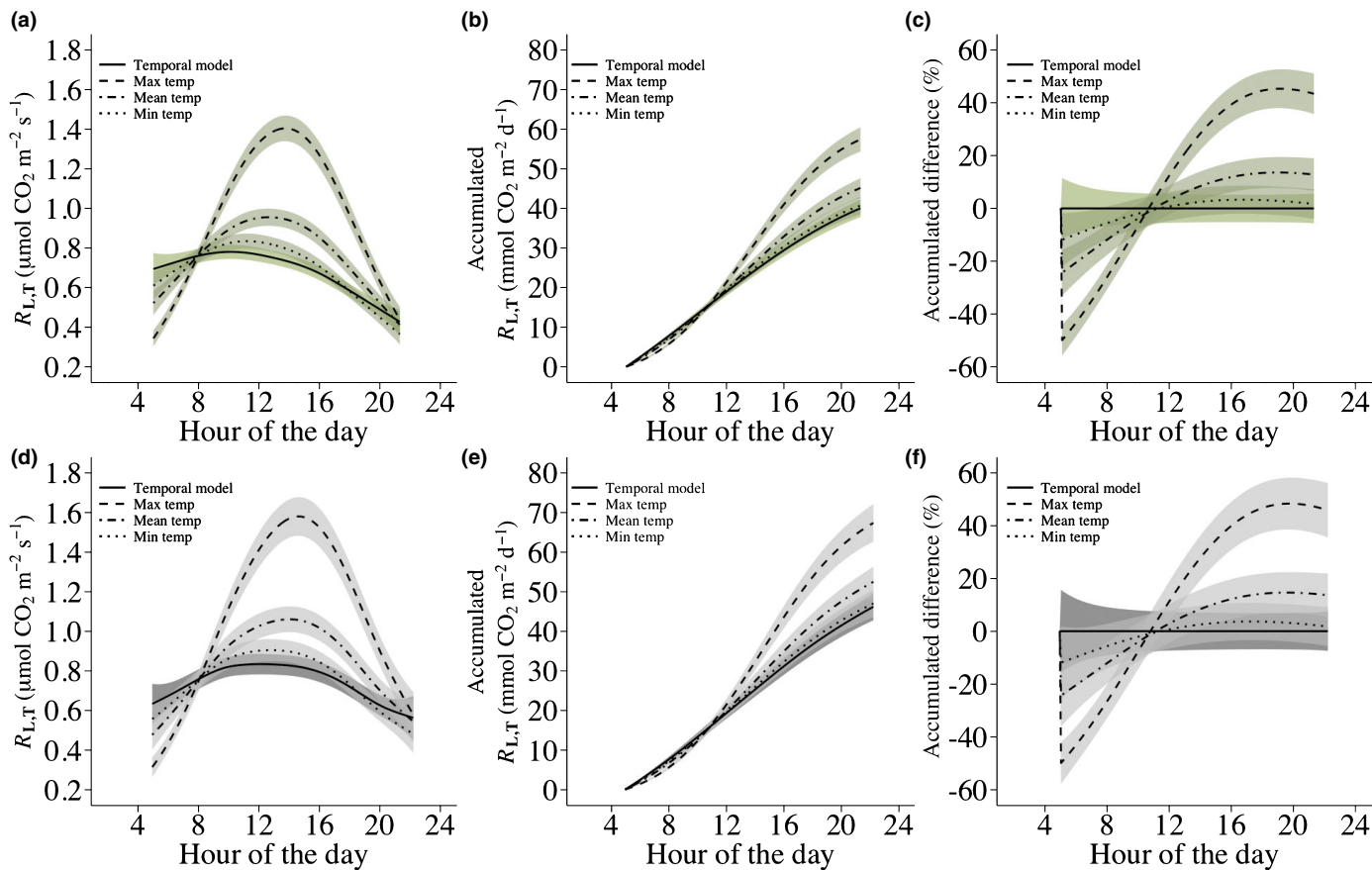
Fig. 4 Temporal generalized additive models (GAMs) of respiration in the light at constant temperature ($R_{L,To}$) (solid line) and maximum, mean and minimum temperature variation models of respiration in the light at varying temperature ($R_{L,T}$) (dashed, dot dashed and dotted lines, respectively) with shaded 95% simultaneous confidence bands for Australia (a) and Denmark (d). For the temporal GAMs, a hypothetical $R_{L,To}$ value of 0.76 µmol CO_2 m^{-2} s^{-1} (i.e. the mean estimated $R_{L,To}$ value across all species in this study) measured at 08:00 h was used to predict $R_{L,To}$ values throughout the day at a constant temperature. The maximum, mean and minimum temperature variation models are based on three temperature profiles and predict $R_{L,T}$. The predictions of $R_{L,T}$ were derived by fitting GAMs to the $R_{L,To}/\overline{R_{L,To}}$ measurements from Australia and Denmark. Subsequently, the hypothetical $R_{L,To}$ value measured at 08:00 h was used to predict $R_{L,T}$ throughout the day at different temperatures from the fitted GAM from Australia as: $R_{L,Ti} = (0.76((0.998728 + f(\text{time}_i) + \epsilon_i)/(0.998728 + f(\text{time}_x) + \epsilon_x)))2^{(T_i - T_o/10)}$ and from the fitted GAM from Denmark as: $R_{L,Ti} = (0.76((1.00074 + f(\text{time}_i) + \epsilon_i)/(1.00074 + f(\text{time}_x) + \epsilon_x)))2^{(T_i - T_o/10)}$, where 0.76 is the $R_{L,To}$ value measured at 08:00 h (time$_x$), ϵ_x is the estimated residual error at 08:00 h, $R_{L,Ti}$ is the predicted rate of respiration at temperatures T_i and time point time$_i$, and ϵ_i is the residual errors at time$_i$. T_o is the temperature at the time where the $R_{L,To}$ value of 0.76 was measured and 2 denotes the factor by which $R_{L,Ti}$ changes for every 10°C temperature change. The temperature profiles were derived from the measured ambient temperature during the time of measuring the light response curves in Australia and can be viewed in Supporting Information Fig. S2. (b, e) Daily accumulated CO_2 efflux predicted by the temporal, maximum temperature, mean temperature and minimum temperature variation models for Australia and Denmark, respectively. (c, f) Percentage difference between accumulated CO_2 predicted by the maximum temperature, mean temperature and minimum temperature variation models and the temporal models for Australia and Denmark, respectively.

R_D (Atkin *et al.*, 2005; Zaragoza-Castells *et al.*, 2007; McLaughlin *et al.*, 2014; Kroner & Way, 2016; Crous *et al.*, 2017b). The light inhibition of R_D has been shown to vary between 0 and 100% when estimated with the Kok and Laisk method (Atkin *et al.*, 2006; Zaragoza-Castells *et al.*, 2007; Crous *et al.*, 2012; Heskel *et al.*, 2013) and sometimes R_L even exceeds R_D (Zaragoza-Castells *et al.*, 2007; Atkin *et al.*, 2013; Crous *et al.*, 2017a) as demonstrated in this study as well for three measurements. Given this variability, approaches where R_L is calculated from measurements of R_D, by assuming R_L constitutes a fixed fraction of R_D (e.g the JULES model), may be erroneous. The light inhibition of $R_{D,To}$ showed only a weak association with the external light intensity above

c. 100 µmol photons m^{-2} s^{-1} in Australia and decreased in a linear fashion with increasing A_{gross} for both Australia and Denmark, as shown previously (Atkin *et al.*, 2013). However, the cause of the large difference in variability of the light inhibition of $R_{D,To}$ between climates, with much higher inhibition values in Denmark, is unknown. Eight out of 10 species were measured in autumn in Denmark where inhibition values have been shown to increase (Heskel *et al.*, 2014) whereas lower inhibition values have been reported earlier in the growing season (Crous *et al.*, 2012; Heskel *et al.*, 2014). Seasonal differences in light inhibition may contribute to the observed variability because the degree of inhibition has been shown to decrease under environmental conditions that increase the

demand for energy and C skeletons, such as elevated CO_2 (Wang *et al.*, 2001; Shapiro *et al.*, 2004) and increased soil nutrient availability (Heskel *et al.*, 2012).

Mechanisms related to the diurnal variation of respiration in the light at constant measuring temperature

Many processes can affect respiratory CO_2 effluxes of leaves in the light (Tcherkez *et al.*, 2017b). These include the oxidative pentose phosphate pathway (Buckley & Adams, 2011; Shameer *et al.*, 2019; Xu *et al.*, 2021), photorespiration (Igamberdiev *et al.*, 2001; Tcherkez *et al.*, 2005, 2008, 2012a), the continued utilization of stored organic acids (Gauthier *et al.*, 2010), the activity of the pyruvate dehydrogenase complex (Budde & Randall, 1990; Gemel & Randall, 1992), the activity of the malic enzyme (Gauthier *et al.*, 2020) and NAD(P)H : NAD(P) ratios (Igamberdiev & Gardeström, 2003). Some CO_2 fluxes may even originate from nonleaf sources that are transported through the vascular tissues to leaves and subsequently released (Stutz *et al.*, 2017; Stutz & Hanson, 2019). It is therefore paramount to study how such processes are temporally coregulated and affect CO_2 effluxes in the light.

The diurnal variation of $R_{L,To}/\overline{R_{L,To}}$ and $R_{D,To}/\overline{R_{D,To}}$ showed a notable consistency throughout the study period. The wide range of measurement temperatures between the days of measuring showed no association with $R_{L,To}/\overline{R_{L,To}}$ and $R_{D,To}/\overline{R_{D,To}}$, and the ambient temperature, VPD and external light intensity above *c.* 100 µmol photons m^{-2} s^{-1} showed only weak associations with $R_{L,To}/\overline{R_{L,To}}$ and $R_{D,To}/\overline{R_{D,To}}$. This does not explicitly imply that variations in these factors were unimportant, but given the consistency of the diurnal patterns, it should be considered whether circadian regulation could play a role. R_D, light-enhanced dark respiration (LEDR) (Gessler *et al.*, 2017), g_s, A_{net} (Hennessey *et al.*, 1993; Dodd *et al.*, 2014) and indirectly R_L (Doughty *et al.*, 2006; Resco de Dios *et al.*, 2012) have been shown to be under circadian control, and further research is needed to shed light on the importance of circadian regulation in leaf daytime respiration.

Previous work has shown that photosynthesis regulates R_L through ATP utilization in sucrose synthesis, redox maintenance and substrate supply (Krömer *et al.*, 1988; Raghavendra *et al.*, 1994; Krömer, 1995; Hoefnagel *et al.*, 1998), and a coupling of R_L to the rate of photosynthesis would explain the association between $R_{L,To}/\overline{R_{L,To}}$ and A_{gross} observed in both Australia and Denmark. The rate of photosynthesis may additionally have influenced the regulation of $R_{D,To}/\overline{R_{D,To}}$ given the effect of accumulated net CO_2 assimilation on R_D due to LEDR (Azcón-Bieto & Osmond, 1983; Hymus *et al.*, 2005; Barbour *et al.*, 2011). The fact that $R_{L,To}/\overline{R_{L,To}}$ and $R_{D,To}/\overline{R_{D,To}}$ exhibited different diurnal patterns within climates may be related to the differential regulation of R_L and R_D (Hurry *et al.*, 2005; Tcherkez *et al.*, 2010, 2017b), and to the participation of photosynthesis in the regulatory process because the availability of substrates for R_L and R_D are influenced by time of day (Pärnik *et al.*, 2002, 2007; Nogués *et al.*, 2004; Pärnik & Keerberg, 2007; Florez-Sarasa *et al.*, 2012; Griffin & Turnbull, 2012).

In this study, stomatal conductance showed a strong association with A_{gross} in Australia. This could indicate an indirect stomatal regulation of $R_{L,To}/\overline{R_{L,To}}$ and $R_{D,To}/\overline{R_{D,To}}$ because of the positive linear relationship between A_{gross} and the two. In Denmark, stomatal conductance showed a weak association with A_{gross} compared to Australia, and A_{gross} only showed a weak positive linear relationship with $R_{L,To}/\overline{R_{L,To}}$ and none with $R_{D,To}/\overline{R_{D,To}}$. This suggests that the difference in the diurnal patterns of $R_{L,To}/\overline{R_{L,To}}$ and $R_{D,To}/\overline{R_{D,To}}$ between Australia and Denmark were an indirect result of stomatal regulation through differences in environmental factors between the climates. The fact that the PFTs measured in Australia exhibited similar diurnal patterns in $R_{L,To}/\overline{R_{L,To}}$ and $R_{D,To}/\overline{R_{D,To}}$ supports this. In addition, the fact that different species were measured in Australia and Denmark also provides a plausible explanation for this phenomenon.

In this study, increased C_i at decreasing irradiance levels was corrected using Eqn 1, but this approach assumes infinite g_m and therefore $C_i = C_c$, which is known to be unlikely under some conditions (Harley *et al.*, 1992; Flexas *et al.*, 2007; Yin & Struik, 2009). In this study, diurnal changes in VPD were presumably much higher in Australia compared to Denmark, thereby making it more likely that g_m and g_s would exhibit asynchronous diurnal patterns in Australia. As a result, the $C_i = C_c$ assumption would be erroneous, which could explain some of the diurnal variation in $R_{L,To}/\overline{R_{L,To}}$ and the light inhibition of $R_{D,To}$ observed in Australia. It thus seems unlikely that the diurnal variation of $R_{L,To}/\overline{R_{L,To}}$ and the light inhibition of $R_{D,To}$ is solely a result of a differential regulation of g_m and g_s.

Accounting for effects of time of day when measuring R_L using the Kok method

This study shows that time of day can have considerable effects on estimates of R_L conducted in the field with the Kok method. Comparisons of R_L between leaves should only be made at the same time of the day with the recognition that leaves may have been exposed to different environmental conditions before being measured. For computing daily averages, measurements should cover the entire photoperiod for a given leaf to yield precise estimates of daily accumulated CO_2 effluxes. Measuring throughout the entire photoperiod is difficult experimentally especially because measurements need to be at the leaf level, which might not be possible in all experimental designs. This study offers a parametric and nonparametric approach whereby an $R_{L,To}$ measurement for a given leaf can be predicted throughout the day at other temperatures using the supplementary EXCEL spreadsheet and R script (Dataset S1; Notes S2) based on Eqns 7 and 8, respectively. The approach can easily be implemented to other models (e.g. V_{cmax}) by inserting the estimated model coefficients from Fig. S15 into Eqn 8. The method assumes R_L follows a distinct relative diurnal pattern (i.e. the predictions may vary in absolute values but not in per cent) regardless of environmental factors other than temperature as well as species and PFTs. Predictions should only be based on R_L measurements derived with the Kok method.

Conclusion

This study demonstrates that R_L, R_D and the light inhibition of R_D exhibit significant diurnal variations when measured with a constant temperature in the field with the Kok method. The diurnal pattern of R_L and R_D differed in trajectory and magnitude between climates but not between PFTs, while it differed both between climates and in trajectory between PFTs for the light inhibition of R_D. The results emphasize that time of day should be accounted for in studies seeking to estimate the response of leaf daytime respiration to variation in other factors (e.g. temperature and species), or when deriving inference across studies. The results highlight the dynamic nature of leaf daytime respiration that are driven by factors other than the measuring temperature and that R_L and R_D exhibit distinct diurnal patterns. Temporal variation in the regulatory relationship between physiological mechanisms and leaf respiration needs further attention to unveil the drivers of leaf respiration.

Author contributions

AHF, DB, JY, KLG, MP and MGT planned and designed the research. AHF performed experiments, conducted field work and analysed the data. AHF and DB drafted the manuscript. All authors contributed to and revised the manuscript.

ORCID

Dan Bruhn https://orcid.org/0000-0002-9811-9194
Andreas H. Faber https://orcid.org/0000-0003-3356-7591
Kevin L. Griffin https://orcid.org/0000-0003-4124-3757
Majken Pagter https://orcid.org/0000-0001-5441-1508
Mark G. Tjoelker https://orcid.org/0000-0003-4607-5238
Jinyan Yang https://orcid.org/0000-0002-4936-0627

Data availability

The data used in this article can be found in the supplementary Excel spreadsheet (Dataset S1) and are publicly available at: 10.6084/m9.figshare.20089256.

References

Amthor JS, Baldocchi DD. 2001. Terrestrial higher plant respiration and net primary productivity. In: Roy J, Saugier B, Mooney H, eds. *Terrestrial global productivity*. San Diego, CA, USA: Academic Press, 33–59.

Atkin OK, Bloomfield KJ, Reich PB, Tjoelker MG, Asner GP, Bonal D, Bönisch G, Bradford MG. 2015. Global variability in leaf respiration in relation to climate, plant functional types and leaf traits. *New Phytologist* 206: 614–636.

Atkin OK, Bruhn D, Hurry VM, Tjoelker MG. 2005. Evans review no. 2: The hot and the cold: unravelling the variable response of plant respiration to temperature. *Functional Plant Biology* 32: 87–105.

Atkin OK, Evans JR, Ball MC, Lambers H, Pons TL. 2000. Leaf respiration of snow gum in the light and dark. Interactions between temperature and irradiance. *Plant Physiology* 122: 915–923.

Atkin OK, Scheurwater I, Pons TL. 2006. High thermal acclimation potential of both photosynthesis and respiration in two lowland *Plantago* species in contrast to an alpine congeneric. *Global Change Biology* 12: 500–515.

Atkin OK, Turnbull MH, Zaragoza-Castells J, Fyllas NM, Lloyd J, Meir P, Griffin KL. 2013. Light inhibition of leaf respiration as soil fertility declines along a post-glacial chronosequence in New Zealand: an analysis using the Kok method. *Plant and Soil* 367: 163–182.

Ayub G, Smith RA, Tissue DT, Atkin OK. 2011. Impacts of drought on leaf respiration in darkness and light in *Eucalyptus saligna* exposed to industrial-age atmospheric CO_2 and growth temperature. *New Phytologist* 190: 1003–1018.

Ayub G, Zaragoza-Castells J, Griffin KL, Atkin OK. 2014. Leaf respiration in darkness and in the light under pre-industrial, current and elevated atmospheric CO_2 concentrations. *Plant Science* 226: 120–130.

Azcón-Bieto J, Osmond CB. 1983. Relationship between photosynthesis and respiration: the effect of carbohydrate status on the rate of CO_2 production by respiration in darkened and illuminated wheat leaves. *Plant Physiology* 71: 574–581.

Barbour MM, Hunt JE, Kodama N, Laubach J, McSeveny TM, Rogers GN, Tcherkez G, Wingate L. 2011. Rapid changes in $\delta^{13}C$ of ecosystem-respired CO_2 after sunset are consistent with transient ^{13}C enrichment of leaf respired CO_2. *New Phytologist* 190: 990–1002.

Bathellier C, Badeck FW, Ghashghaie J. 2017. Carbon isotope fractionation in plant respiration. In: Tcherkez G, Ghashghaie J, eds. *Plant respiration: metabolic fluxes and carbon balance. Advances in photosynthesis and respiration*. Cham, Switzerland: Springer, 43–68.

Bolstad PV, Reich P, Lee T. 2003. Rapid temperature acclimation of leaf respiration rates in *Quercus alba* and *Quercus rubra*. *Tree Physiology* 23: 969–976.

Brooks A, Farquhar GD. 1985. Effect of temperature on the CO_2/O_2 specificity of ribulose-1,5-bisphosphate carboxylase/oxygenase and the rate of respiration in the light. *Planta* 165: 397–406.

Bruhn D, Mikkelsen TN, Herbst M, Kutsch WL, Ball MC, Pilegaard K. 2011. Estimating daytime ecosystem respiration from eddy-flux data. *Biosystems* 103: 309–313.

Buckley TN, Adams MA. 2011. An analytical model of non-photorespiratory CO_2 release in the light and dark in leaves of C_3 species based on stoichiometric flux balance. *Plant, Cell & Environment* 34: 89–112.

Buckley TN, Vice H, Adams MA. 2017. The Kok effect in *Vicia faba* cannot be explained solely by changes in chloroplastic CO_2 concentration. *New Phytologist* 216: 1064–1071.

Budde RJA, Randall D. 1990. Pea leaf mitochondrial pyruvate dehydrogenase complex is inactivated *in vivo* in a light-dependent manner. *Proceedings of the National Academy of Sciences, USA* 87: 673–676.

von Caemmerer S, Farquhar G. 1981. Some relationships between the biochemistry of photosynthesis and the gas exchange of leaves. *Planta* 153: 376–387.

Canadell JG, Le Quéré C, Raupach MR, Field CB, Buitenhuis ET, Ciais P, Conway TJ, Gillett NP, Houghton RA, Marland G *et al.* 2007. Contributions to accelerating atmospheric CO_2 growth from economic activity, carbon intensity, and efficiency of natural sinks. *Proceedings of the National Academy of Sciences, USA* 104: 18866–18870.

Clark DB, Mercado LM, Sitch S, Jones CD, Gedney N, Best MJ, Pryor M, Rooney GG, Essery RLH, Blyth E *et al.* 2011. The Joint UK Land Environment Simulator (JULES), model description – part 2: carbon fluxes and vegetation dynamics. *Geoscientific Model Development* 4: 701–722.

Cox PM. 2001. *Description of the "TRIFFID" dynamic global vegetation model*. Hadley Centre Technical Note 24. Bracknell, UK: Met Office.

Crous KY, O'Sullivan OS, Zaragoza-Castells J, Bloomfield KJ, Negrini ACA, Meir P, Turnbull MH, Griffin KL, Atkin OK. 2017a. Nitrogen and

phosphorus availabilities interact to modulate leaf trait scaling relationships across six plant functional types in a controlled-environment study. *New Phytologist* 215: 992–1008.

Crous KY, Wallin G, Atkin OK, Uddling J, Ekenstam AA. 2017b. Acclimation of light and dark respiration to experimental and seasonal warming are mediated by changes in leaf nitrogen in *Eucalyptus globulus*. *Tree Physiology* 37: 1069–1083.

Crous KY, Zaragoza-Castells J, Ellsworth DS, Duursma RA, Löw M, Tissue DT, Atkin OK. 2012. Light inhibition of leaf respiration in field-grown *Eucalyptus saligna* in whole-tree chambers under elevated atmospheric CO_2 and summer drought. *Plant, Cell & Environment* 35: 966–981.

Curtis CJ, Simpson GL. 2014. Trends in bulk deposition of acidity in the UK, 1988–2007, assessed using additive models. *Ecological Indicators* 37: 274–286.

De Kauwe MG, Lin Y, Wright IJ, Medlyn BE, Crous KY, Ellsworth DS, Maire V, Prentice IC, Atkin OK, Rogers A *et al*. 2016. A test of the 'one-point method' for estimating maximum carboxylation capacity from field-measured, light-saturated photosynthesis. *New Phytologist* 210: 1130–1144.

Dodd AN, Kusakina J, Hall A, Gould PD, Hanaoka M. 2014. The circadian regulation of photosynthesis. *Photosynthesis Research* 119: 181–190.

Doughty CE, Goulden ML, Miller SD, da Rocha HR. 2006. Circadian rhythms constrain leaf and canopy gas exchange in an Amazonian forest. *Geophysical Research Letters* 33: L15404.

Drake JE, Tjoelker MG, Aspinwall MJ, Reich PB, Barton CVM, Medlyn BE, Duursma RA. 2016. Does physiological acclimation to climate warming stabilize the ratio of canopy respiration to photosynthesis? *New Phytologist* 211: 850–863.

Farquhar GD, Busch FA. 2017. Changes in the chloroplastic CO_2 concentration explain much of the observed Kok effect. *New Phytologist* 214: 570–584.

Flexas J, Diaz-Espejo A, Galmes J, Kaldenhoff R, Medrano H, Ribas-Carbo M. 2007. Rapid variations of mesophyll conductance in response to changes in CO_2 concentration around leaves. *Plant, Cell & Environment* 30: 1284.

Florez-Sarasa I, Araújo WL, Wallström SV, Rasmusson AG, Fernie AR, Ribas-Carbo M. 2012. Light-responsive metabolite and transcript levels are maintained following a dark-adaptation period in leaves of *Arabidopsis thaliana*. *New Phytologist* 195: 136–148.

Friedlingstein P, O'Sullivan M, Jones MW, Anew RM, Hauck J, Olsen A, Peters GP, Peters W, Pongratz J, Sitch S *et al*. 2020. Global Carbon Budget 2020. *Earth System Science Data* 12: 3269–3340.

Gauthier PPG, Bligny R, Gout E, Mahé A, Nogués S, Hodges M, Tcherkez GGB. 2010. *In folio* isotopic tracing demonstrates that nitrogen assimilation into glutamate is mostly independent from current CO_2 assimilation in illuminated leaves of *Brassica napus*. *New Phytologist* 185: 988–999.

Gauthier PPG, Saenz N, Griffin KL, Way D, Tcherkez GGB. 2020. Is the Kok effect a respiratory phenomenon? Metabolic insight using ^{13}C labeling in *Helianthus annuus* leaves. *New Phytologist* 228: 1243–1255.

Gemel J, Randall DD. 1992. Light regulation of leaf mitochondrial pyruvate dehydrogenase complex: role of photorespiratory carbon metabolism. *Plant Physiology* 100: 908–914.

Gessler A, Roy J, Kayler Z, Ferrio JP, Alday JG, Bahn M, del Castillo J, Devidal S, García-Muñoz S, Landais D *et al*. 2017. Night and day – circadian regulation of night-time dark respiration and light-enhanced dark respiration in plant leaves and canopies. *Environmental and Experimental Botany* 137: 14–25.

Gifford R. 2003. Plant respiration in productivity models: conceptualisation, representation and issues for global terrestrial carbon-cycle research. *Functional Plant Biology* 30: 171–186.

Griffin KL, Turnbull MH. 2012. Out of the light and into the dark: post-illumination respiratory metabolism. *New Phytologist* 195: 4–7.

Griffin KL, Turnbull MH. 2013. Light saturated RuBP oxygenation by Rubisco is a robust predictor of light inhibition of respiration in *Triticum aestivum* L. *Plant Biology* 15: 769–775.

Hagedorn F, Joseph J, Peter M, Luster J, Pritsch K, Geppert U, Kerner R, Molinier V, Egli S, Schaub M *et al*. 2016. Recovery of trees from drought depends on belowground sink control. *Nature Plants* 2: 16111.

Harley PC, Loreto F, Di Marco G, Sharkey TD. 1992. Theoretical considerations when estimating the mesophyll conductance to CO_2 flux by analysis of the response of photosynthesis to CO_2. *Plant Physiology* 98: 1429–1436.

Hennessey TL, Freeden AL, Field CB. 1993. Environmental effects of circadian rhythms in photosynthesis and stomatal opening. *Planta* 189: 369–376.

Heskel MA, Anderson OR, Atkin OK, Turnbull MH, Griffin KL. 2012. Leaf- and cell-level carbon cycling responses to a nitrogen and phosphorus gradient in two Arctic tundra species. *American Journal of Botany* 99: 1702–1714.

Heskel MA, Atkin OK, Turnbull MH, Griffin KL. 2013. Bringing the Kok effect to light: a review on the integration of daytime respiration and net ecosystem exchange. *Ecosphere* 4: art98-14.

Heskel MA, Bitterman D, Atkin OK, Turnbull MH, Griffin KL. 2014. Seasonality of foliar respiration in two dominant plant species from the Arctic tundra: response to long-term warming and short-term temperature variability. *Functional Plant Biology* 42: 287–300.

Hoefnagel MHN, Atkin OK, Wiskich JT. 1998. Interdependence between chloroplasts and mitochondria in the light and the dark. *Biochimica et Biophysica Acta (BBA) – Bioenergetics* 1366: 235–255.

Högberg P, Read DJ. 2006. Towards a more plant physiological perspective on soil ecology. *Trends in Ecology & Evolution* 21: 548–554.

Huntingford C, Zelazowski P, Galbraith D, Mercado LM, Sitch S, Fisher R, Lomas M, Walker AP, Jones CD, Booth BBB *et al*. 2013. Simulated resilience of tropical rainforests to CO_2-induced climate change. *Nature Geoscience* 6: 268–273.

Hurry V, Igamberdiev AU, Keerberg O, Pärnik T, Atkin OK, Zaragoza-Castells J, Gardeström P. 2005. Respiration in photosynthetic cells: gas exchange components, interactions with photorespiration and the operation of mitochondria in the light. In: *Advances in photosynthesis and respiration. Plant respiration*. Dordrecht, the Netherlands: Springer, 43–61.

Hymus G, Maseyk K, Valentini R, Yakir D. 2005. Large daily variation in ^{13}C-enrichment of leaf-respired CO_2 in two *Quercus* forest canopies. *New Phytologist* 167: 377–384.

Igamberdiev AU, Gardeström P. 2003. Regulation of NAD- and NADP-dependent isocitrate dehydrogenases by reduction levels of pyridine nucleotides in mitochondria and cytosol of pea leaves. *Biochimica et Biophysica Acta (BBA) – Bioenergetics* 1606: 117–125.

Igamberdiev AU, Romanowska E, Gardeström P. 2001. Photorespiratory flux and mitochondrial contribution to energy and redox balance of barley leaf protoplasts in the light and during light–dark transitions. *Journal of Plant Physiology* 158: 1325–1332.

Janssens IA, Lankreijer H, Matteucci G, Kowalski AS, Buchmann N, Epron D, Pilegaard K, Kutsch W, Longdoz B, Grünwald T *et al*. 2001. Productivity overshadows temperature in determining soil and ecosystem respiration across European forests. *Global Change Biology* 7: 269–278.

Kirschbaum MUF, Farquhar GD. 1987. Investigation of the CO_2 dependence of quantum yield and respiration in *Eucalyptus pauciflora*. *Plant Physiology* 83: 1032–1036.

Kok B. 1948. A critical consideration of the quantum yield of *Chlorella* photosynthesis. *Enzymologia* 13: 1–56.

Kornfeld A, Heskel M, Atkin OK, Gough L, Griffin KL, Horton TW, Turnbull MH. 2013. Respiratory flexibility and efficiency are affected by simulated global change in Arctic plants. *New Phytologist* 197: 1161–1172.

Krömer S. 1995. Respiration during photosynthesis. *Annual Review of Plant Physiology and Plant Molecular Biology* 46: 45–70.

Krömer S, Stitt M, Heldt H. 1988. Mitochondrial oxidative phosphorylation participating in photosynthetic metabolism of a leaf cell. *FEBS Letters* 226: 352–356.

Kroner Y, Way DA. 2016. Carbon fluxes acclimate more strongly to elevated growth temperatures than to elevated CO_2 concentrations in a northern conifer. *Global Change Biology* 22: 2913–2928.

Kruse J, Rennenberg H, Adams MA. 2011. Steps towards a mechanistic understanding of respiratory temperature responses. *New Phytologist* 189: 659–677.

Le Quéré C, Canadell JG, Marland G, Raupach MR. 2009. Trends in the sources and sinks of carbon dioxide. *Nature Geoscience* 2: 831–836.

Leuzinger S, Thomas RQ. 2011. How do we improve Earth system models? Integrating Earth system models, ecosystem models, experiments and long-term data. *New Phytologist* 191: 15–18.

Lombardozzi DL, Bonan GB, Smith NG, Dukes JS, Fisher RA. 2015. Temperature acclimation of photosynthesis and respiration: a key uncertainty

in the carbon cycle-climate feedback. *Geophysical Research Letters* **42**: 8624–8631.

Loveys BR, Atkinson LJ, Sherlock DJ, Roberts RL, Fitter AH, Atkin OK. 2003. Thermal acclimation of leaf and root respiration: an investigation comparing inherently fast- and slow-growing plant species. *Global Change Biology* **9**: 895–910.

McLaughlin BC, Xu C-Y, Rastetter EB, Griffin KL. 2014. Predicting ecosystem carbon balance in a warming Arctic: the importance of long-term thermal acclimation potential and inhibitory effects of light on respiration. *Global Change Biology* **20**: 1901–1912.

Melillo JM, McGuire AD, Kicklighter DW, Moore B, Vorosmarty CJ, Schloss AL. 1993. Global climate change and terrestrial net primary production. *Nature* **363**: 234–240.

Morgenstern K, Andrew Black T, Humphreys ER, Griffis TJ, Drewitt GB, Cai T, Nesic Z, Spittlehouse DL, Livingston NJ. 2004. Sensitivity and uncertainty of the carbon balance of a Pacific Northwest Douglas-fir forest during an El Niño/La Niña cycle. *Agricultural and Forest Meteorology* **123**: 201–219.

Nogués S, Tcherkez G, Cornic G, Ghashghaie J. 2004. Respiratory carbon metabolism following illumination in intact French bean leaves using $^{13}C/^{12}C$ isotope labeling. *Plant Physiology* **136**: 3245–3254.

O'Leary BM, Asao S, Millar AH, Atkin OK. 2019. Core principles which explain variation in respiration across biological scales. *New Phytologist* **222**: 670–686.

Oleson K, Lawrence DM, Bonan GB, Drewniak B, Huang M, Koven CD, Levis S, Li F, Riley WJ, Subin ZM et al. 2013. *Technical description of v.4.5 of the Community Land Model (CLM) (no. NCAR/TN-503+ STR).* Boulder, CO, USA: National Center for Atmospheric Research, 422.

Pärnik T, Ivanova H, Keerberg O. 2007. Photorespiratory and respiratory decarboxylations in leaves of C₃ plants under different CO₂ concentrations and irradiances. *Plant, Cell & Environment* **30**: 1535–1544.

Pärnik T, Keerberg O. 2007. Advanced radiogasometric method for the determination of the rates of photorespiratory and respiratory decarboxylations of primary and stored photosynthates under steady-state photosynthesis. *Physiologia Plantarum* **129**: 34–44.

Pärnik TR, Voronin PY, Ivanova HN, Keerberg OF. 2002. Respiratory CO₂ fluxes in photosynthesizing leaves of C₃ species varying in rates of starch synthesis. *Russian Journal of Plant Physiology* **49**: 729–735.

Pinheiro JC, Bates D. 2000. *Mixed-effects models in S and S-PLUS.* New York, NY, USA: Springer Science & Business Media.

Prentice IC, Farquhar GD, Fasham MJR, Goulden ML, Heimann M, Jaramillo VJ, Kheshgi HS, Le Quéré C, Scholes RJ, Wallace DWR. 2001. The carbon cycle and atmospheric carbon dioxide. In: Houghton JT, Ding Y, Griggs DG, Noguer M, Van Der Linden PJ, Dai X, Maskell K, Johnson CA, eds. *Climate change 2001: the scientific basis. Contribution of working group I to the 3rd assessment report of the IPCC.* Cambridge, UK: Cambridge University Press, 183–238.

R Core Team. 2021. *R: a language and environment for statistical computing. v.4.1.0.* Vienna, Austria: R Foundation for Statistical Computing.

R Studio Team. 2021. *Rstudio: integrated development environment for R. v.1.4.1717.* Boston, MA, USA: RStudio, PBC.

Raghavendra AS, Padmasree K, Saradadevi K. 1994. Interdependence of photosynthesis and respiration in plant cells – interactions between chloroplasts and mitochondria. *Plant Science* **97**: 1–14.

Raich JW, Rastetter EB, Melillo JM, Kicklighter DW, Studler PA, Peterson BJ, Grace AL, Moore B III, Vorosmarty CJ. 1991. Potential net primary productivity in South America: application of a global model. *Ecological Applications* **1**: 399–429.

Reich PB, Walters MB, Tjoelker MG, Vanderklein D, Buschena C. 1998. Photosynthesis and respiration rates depend on leaf and root morphology and nitrogen concentration in nine boreal tree species differing in relative growth rate. *Functional Ecology* **12**: 395–405.

Resco de Dios V, Gessler A. 2018. Circadian regulation of photosynthesis and transpiration from genes to ecosystems. *Environmental and Experimental Botany* **152**: 37–48.

Resco de Dios V, Goulden ML, Ogle K, Richardson AD, Hollinger DY, Davidson EA, Alday JG, Barron-Gafford GA, Carrara A, Kowalski AS et al.

2012. Endogenous circadian regulation of carbon dioxide exchange in terrestrial ecosystems. *Global Change Biology* **18**: 1956–1970.

Running SW, Coughlan JC. 1988. A general model of forest ecosystem processes for regional applications I. Hydrologic balance, canopy gas exchange and primary production processes. *Ecological Modelling* **42**: 125–154.

Searle SY, Thomas S, Griffin KL, Horton T, Kornfeld A, Yakir D, Hurry V, Turnbull MH. 2011. Leaf respiration and alternative oxidase in field-grown alpine grasses respond to natural changes in temperature and light. *New Phytologist* **189**: 1027–1039.

Shameer S, Ratcliffe RG, Sweetlove LJ. 2019. Leaf energy balance requires mitochondrial respiration and export of chloroplast NADPH in the light. *Plant Physiology* **180**: 1947–1961.

Shapiro JB, Griffin KL, Lewis JD, Tissue DT. 2004. Response of *Xanthium strumarium* leaf respiration in the light to elevated CO₂ concentration, nitrogen availability and temperature. *New Phytologist* **162**: 377–386.

Simpson GL. 2018. Modelling palaeoecological time series using generalised additive models. *Frontiers in Ecology and Evolution* **6**: 149.

Slot M, Wright SJ, Kitajima K. 2013. Foliar respiration and its temperature sensitivity in trees and lianas: *in situ* measurements in the upper canopy of a tropical forest. *Tree Physiology* **33**: 505–515.

Smith NG, Dukes JS. 2013. Plant respiration and photosynthesis in global-scale models: incorporating acclimation to temperature and CO₂. *Global Change Biology* **19**: 45–63.

Sperlich D, Barbeta A, Ogaya R, Sabate S, Penuelas J. 2016. Balance between carbon gain and loss under long-term drought: impacts on foliar respiration and photosynthesis in *Quercus ilex* L. *Journal of Experimental Botany* **67**: 821–833.

Stutz SS, Anderson J, Zulick R, Hanson DT. 2017. Inside out: efflux of carbon dioxide from leaves represents more than leaf metabolism. *Journal of Experimental Botany* **68**: 2849–2857.

Stutz SS, Hanson DT. 2019. Contribution and consequences of xylem-transported CO₂ assimilation for C₃ plants. *New Phytologist* **223**: 1230–1240.

Tcherkez G, Bligny R, Gout E, Mahé A, Hodges M, Cornic G. 2008. Respiratory metabolism of illuminated leaves depends on CO and O conditions. *Proceedings of the National Academy of Sciences, USA* **105**: 797–802.

Tcherkez G, Boex-Fontvieille E, Mahé A, Hodges M. 2012a. Respiratory carbon fluxes in leaves. *Current Opinion in Plant Biology* **15**: 308–314.

Tcherkez G, Cornic G, Bligny R, Gout E, Ghashghaie J. 2005. *In vivo* respiratory metabolism of illuminated leaves. *Plant Physiology* **138**: 1596–1606.

Tcherkez G, Gauthier P, Buckley TN, Busch FA, Barbour MM, Bruhn D, Heskel MA, Gong XY, Crous K, Griffin KL et al. 2017a. Tracking the origins of the Kok effect, 70 years after its discovery. *New Phytologist* **214**: 506–510.

Tcherkez G, Gauthier P, Buckley TN, Busch FA, Barbour MM, Bruhn D, Heskel MA, Gong XY, Crous KY, Griffin K et al. 2017b. Leaf day respiration: low CO₂ flux but high significance for metabolism and carbon balance. *New Phytologist* **216**: 986–1001.

Tcherkez G, Mahé A, Gauthier P, Mauve C, Gout E, Bligny R, Cornic G, Hodges M. 2009. In folio respiratory fluxomics revealed by ^{13}C isotopic labeling and H/D isotope effects highlight the noncyclic nature of the tricarboxylic acid 'cycle' in illuminated leaves. *Plant Physiology* **151**: 620–630.

Tcherkez G, Mahé A, Guérard F, Boex-Fontvieille ERA, Gout E, Lamothe M, Barbour MM, Bligny R. 2012b. Short-term effects of CO₂ and O₂ on citrate metabolism in illuminated leaves. *Plant, Cell & Environment* **35**: 2208–2220.

Tcherkez G, Schäufele R, Nogués S, Piel C, Broom A, Lanigan G, Barbaroux C, Mata C, Elhani S, Hemming D et al. 2010. On the $^{13}C/^{12}C$ isotopic signal of day and night respiration at the mesocosm level. *Plant, Cell & Environment* **33**: 900–913.

Tjoelker MG, Craine JM, Wedin D, Reich PB, Tilman D. 2005. Linking leaf and root trait syndromes among 39 grassland and savanna species. *New Phytologist* **167**: 493–508.

Trumbore S. 2006. Carbon respired by terrestrial ecosystems – recent progress and challenges. *Global Change Biology* **12**: 141–153.

Turnbull MH, Tissue DT, Griffin KL, Richardson SJ, Peltzer DA, Whitehead D. 2005. Respiration characteristics in temperate rainforest tree species differ along a long-term soil-development chronosequence. *Oecologia* **143**: 271–279.

Villar R, Held A, Merino J. 1994. Comparison of methods to estimate dark respiration in the light in leaves of two woody species. *Plant Physiology* **105**: 167–172.

Wang X, Lewis JD, Tissue DT, Seemann JR, Griffin KL. 2001. Effects of elevated atmospheric CO_2 concentration on leaf dark respiration of *Xanthium strumarium* in light and in darkness. *Proceedings of the National Academy of Sciences, USA* **98**: 2479–2484.

Way DA, Aspinwall MJ, Drake JE, Crous KY, Campany CE, Ghannoum O, Tissue DT, Tjoelker MG. 2019. Responses of respiration in the light to warming in field-grown trees: a comparison of the thermal sensitivity of the Kok and Laisk methods. *New Phytologist* **222**: 132–143.

Way DA, Holly C, Bruhn D, Ball MC, Atkin OK. 2015. Diurnal and seasonal variation in light and dark respiration in field-grown *Eucalyptus pauciflora. Tree Physiology* **35**: 840–849.

Way DA, Yamori W. 2014. Thermal acclimation of photosynthesis: on the importance of adjusting our definitions and accounting for thermal acclimation of respiration. *Photosynthesis Research* **119**: 89–100.

Weerasinghe LK, Creek D, Crous KY, Xiang S, Liddell MJ, Turnbull MH, Atkin OK. 2014. Canopy position affects the relationships between leaf respiration and associated traits in a tropical rainforest in Far North Queensland. *Tree Physiology* **34**: 564–584.

Wieling M. 2018. Analyzing dynamic phonetic data using generalized additive mixed modeling: a tutorial focusing on articulatory differences between L1 and L2 speakers of English. *Journal of Phonetics* **70**: 86–116.

Wijnen H, Young MW. 2006. Interplay of circadian clocks and metabolic rhythms. *Annual Review of Genetics* **40**: 409–448.

Wohlfahrt G, Bahn M, Haslwanter A, Newesely C, Cernusca A. 2005. Estimation of daytime ecosystem respiration to determine gross primary production of a mountain meadow. *Agricultural and Forest Meteorology* **130**: 13–25.

Wood SN. 2017. *Generalized additive models: an introduction with R.* Boca Raton, FL, USA: CRC Press.

Xiang S, Reich PB, Sun S, Atkin OK, Turnbull M. 2013. Contrasting leaf trait scaling relationships in tropical and temperate wet forest species. *Functional Ecology* **27**: 522–534.

Xu Y, Fu X, Sharkey TD, Shachar-Hill Y, Walker BJ. 2021. The metabolic origins of non-photorespiratory CO_2 release during photosynthesis: a metabolic flux analysis. *Plant Physiology* **186**: 297–314.

Yin X, Niu Y, van der Putten PE, Struik PC. 2020. The Kok effect revisited. *New Phytologist* **227**: 1764–1775.

Yin X, Struik P. 2009. Theoretical reconsiderations when estimating the mesophyll conductance to CO_2 diffusion in leaves of C_3 plants by analysis of combined gas exchange and chlorophyll fluorescence measurements. *Plant, Cell & Environment* **32**: 1513–1524.

Yin X, Sun Z, Struik PC, Gu J. 2011. Evaluating a new method to estimate the rate of leaf respiration in the light by analysis of combined gas exchange and chlorophyll fluorescence measurements. *Journal of Experimental Botany* **62**: 3489–3499.

Zaragoza-Castells J, Sánchez-Gómez D, Valladares F, Hurry V, Atkin OK. 2007. Does growth irradiance affect temperature dependence and thermal acclimation of leaf respiration? Insights from a Mediterranean tree with long-lived leaves. *Plant, Cell & Environment* **30**: 820–833.

Supporting Information

Additional Supporting Information may be found online in the Supporting Information section at the end of the article.

Dataset S1 EXCEL spreadsheet containing the data used in this study including a guide on how to calculate $R_{L,T}$ throughout the day by taking into account the temporal variation in $R_{L,To}$ using the supplemented R script.

Fig. S1 Example of a light response curve of measured and C_i-corrected leaf net CO_2 exchange measurements plotted against photosynthetically active radiation.

Fig. S2 Mean ambient temperature (°C) during the time of measuring the light response curves in Australia with fitted quadratic linear regression models depicting the maximum, mean and minimum temperature profiles.

Fig. S3 Diurnal variation of leaf respiration in the light ($R_{L,To}$) and leaf dark respiration ($R_{D,To}$) from Australia and Denmark.

Fig. S4 Leaf respiration in the light ($R_{L,To}/\overline{R_{L,To}}$) and leaf dark respiration ($R_{D,To}/\overline{R_{D,To}}$) measurements across Australia and Denmark plotted against the preset leaf measuring temperature during the time of measuring the light response curves of each leaf.

Fig. S5 Diurnal variation of leaf respiration in the light, $R_{L,To}/\overline{R_{L,To}}$, and leaf dark respiration, $R_{D,To}/\overline{R_{D,To}}$, of *Solanum nigrum, Eucalyptus saligna, Eucalyptus tereticornis* and *Eucalyptus parramattensis* from Australia with fitted generalized additive models.

Fig. S6 Diurnal variation of leaf respiration in the light, $R_{L,To}/\overline{R_{L,To}}$, and leaf dark respiration, $R_{D,To}/\overline{R_{D,To}}$, of *Carya illinoinensis, Dichondra repens, Eucalyptus camaldulensis* and *Araujia sericifera* from Australia with fitted generalized additive models.

Fig. S7 Diurnal variation of leaf respiration in the light, $R_{L,To}/\overline{R_{L,To}}$, and leaf dark respiration, $R_{D,To}/\overline{R_{D,To}}$, of *Malus domestica, Liriodendron tulipifera* and *Platanus acerifolia* from Australia with fitted generalized additive models.

Fig. S8 Diurnal variation of leaf respiration in the light, $R_{L,To}/\overline{R_{L,To}}$, and leaf dark respiration, $R_{D,To}/\overline{R_{D,To}}$, of *Betula pendula, Quercus robur, Fraxinus excelsior* and *Salix cinerea* from Denmark with fitted generalized additive models.

Fig. S9 Diurnal variation of leaf respiration in the light, $R_{L,To}/\overline{R_{L,To}}$, and leaf dark respiration, $R_{D,To}/\overline{R_{D,To}}$, of *Alnus viridis, Alnus glutinosa, Helianthus annus* and *Corylus avellana* from Denmark with fitted generalized additive models.

Fig. S10 Diurnal variation of leaf respiration in the light, $R_{L,To}/\overline{R_{L,To}}$, and leaf dark respiration, $R_{D,To}/\overline{R_{D,To}}$, of *Cornus sanguinea* and *Malus sylvestris* from Denmark with fitted generalized additive models.

Fig. S11 A_{gross} at 100 µmol photons m^{-2} s^{-1} irradiance conducted in Australia and Denmark plotted against g_{sw} at 100 µmol photons m^{-2} s^{-1} irradiance.

Fig. S12 Light inhibition of respiration measurements conducted in Australia and Denmark plotted against A_{gross} at 100 µmol photons m^{-2} s^{-1} irradiance, and against the ambient light intensity.

Fig. S13 Leaf respiration in the light ($R_{L,To}/\overline{R_{L,To}}$) and leaf dark respiration ($R_{D,To}/\overline{R_{D,To}}$) measurements conducted in Australia plotted against the recorded mean ambient temperature (°C) during the time of measuring the light response curves.

Fig. S14 Leaf respiration in the light ($R_{L,To}/\overline{R_{L,To}}$) and leaf dark respiration ($R_{D,To}/\overline{R_{D,To}}$) measurements conducted in Australia plotted against the recorded mean ambient vapour pressure deficit (kPa) during the time of measuring the light response curves.

Fig. S15 Temporal quadratic linear regression models of respiration in the light at constant temperature ($R_{L,To}$) and maximum, mean and minimum temperature variation models of respiration in the light at varying temperature ($R_{L,T}$) for Australia and Denmark, respectively.

Notes S1 Supplementary site description: precipitation and temperature data from 2011 to 2021 and during the time of data collection for the region covering the Danish study sites and the study site in Australia.

Notes S2 R code to calculate temporal patterns of $R_{L,T}$ while accounting for temporal variations in $R_{L,To}$.

Table S1 Measured species in Denmark and Australia with individuals from three different plant functional types (PFTs) (deciduous, herbaceous and evergreen).

Table S2 Total diurnal variation (%) of generalized additive models fitted to $R_{L,To}/\overline{R_{L,To}}$, $R_{D,To}/\overline{R_{D,To}}$ and % light inhibition of $R_{D,To}$ measurements in Fig. 1 that are driven by factors other than the measured temperature.

Table S3 Model comparison between generalized additive models fitted across all $R_{L,To}/\overline{R_{L,To}}$, $R_{D,To}/\overline{R_{D,To}}$ or the light inhibition of $R_{D,To}$ measurements from Australia and Denmark (across climates) with time as the predictor variable (model 1) and a model where climate (across climates) or PFT (across PFTs) was added as a covariate (model 2) or an interaction term (model 3).

Table S4 Mean and variation in the data points of the five light inhibitions of $R_{D,To}$ in Fig. 1(e,f).

Please note: Wiley Blackwell are not responsible for the content or functionality of any Supporting Information supplied by the authors. Any queries (other than missing material) should be directed to the *New Phytologist* Central Office.